City Research Online

City, University of London Institutional Repository

Dynamic stiffness formulation for composite Mindlin plates for exact modal analysis of structures. Part II: Results and applications

M. Boscolo*, J. R. Banerjee

School of Engineering and Mathematical Sciences, City University London, Northampton Square, London, EC1V 0HB

Abstract

The dynamic stiffness method for composite plate elements based on the first order shear deformation theory is implemented in a program called DySAP to compute exact natural frequencies and mode shapes of composite structures. After extensive validation of results using published literature, DySAP is subsequently used to carry out exact free vibration analysis of composite stringer panels. For each example, a finite element solution using NASTRAN is provided and commented on. It is concluded that the dynamic stiffness method is more accurate and computational efficient in free vibration analysis than the traditionally used finite element method.

Keywords: Dynamic stiffness method, thin-walled structures, free vibration analysis, plates, composites.

---

*Corresponding author
Email address: marco.boscolo.1@city.ac.uk (M. Boscolo)

1. INTRODUCTION

The investigation of free vibration behaviour of thin-walled composite structures plays an important role in structural design. Amongst many other applications, the natural frequencies and mode shapes are essentially required to avoid resonance, to predict the dynamic response and to study sound transmission. For thin composite structures, bending or out of plane vibration occurs at relatively lower frequencies than the inplane or membrane ones. For this reason, bending vibration has been extensively covered in the literature [1].

Although out of plane vibrations are of great importance, inplane vibrations can also be important for various applications, e.g. sound transmission, plate systems transmitting inplane forces, or plates subjected to tangential forces, such as the ones produced by the boundary flow of a fluid. Despite this, in plane free vibration analysis of plates has received relatively little attention in the literature. For isotropic plates, in plane free vibration has only recently been studied with some success in [2–5] and in particular, using the dynamic stiffness method [6]. Far less attention has been paid to inplane free vibration of composite plates. A recent contribution to the literature on the subject is by Woodcock et al. [7] where the Rayleigh-Ritz method is used to compute the natural frequencies of a single layer composite square plate for different ply orientations.

For thick composite plates, bending and inplane modes can both occur within the first 10 natural frequencies. It is thus instructive that both of the two motions are studied together. No publication in the literature has so far been identified which deals with both bending and inplane free vibrations of com-

posite plates in an exact manner, particularly including shear deformation and rotatory inertia.

The essential purpose of this two-part paper is not to show in particular, how much difference the effects of shear deformation and rotatory inertia makes to the natural frequencies and mode shapes of a laminated composite plate when using the first order shear deformation theory as opposed to classical plate theory because there are literally dozens of papers in the literature dealing with this subject which have made such assessments [8–18]. It is obviously clear and well known from published literature that the effects could be significant, particularly for thick composite plates, and the importance of the topic becomes even more acute because fibre reinforced composites having low shear modulii are sensitive to the shear deformation effects, unlike isotropic materials. The main purpose of this paper is thus to give a new methodology to deal with the free vibration problems of laminated composite plates using the dynamic stiffness method based on the first order shear deformation theory as a more accurate and efficient alternative to the commonly used finite element method (FEM) [19] rather than pin-pointing the difference in results when using classical plate theory (CPT).

In Part I [20] of this two part paper, a more efficient method to investigate the free vibration behaviour of composite plates has been presented. This method is the dynamic stiffness method (DSM) which has been developed for laminated plates based on the first order shear deformation theory for both bending and inplane vibration. The theory has been implemented in a computer program called DySAP, written in MATLAB enabling the computation of exact natural frequencies and mode shapes of complex structures

3

modelled as composite plate assemblies.

In this second part, attention is focused on results. First the dynamic stiffness elements presented in [20] are validated against exact results available in the literature. This has been possible for simple square or rectangular composite plates. In order to demonstrate the efficiency and accuracy of the present method, the results are also compared to approximate solutions obtained by the commercially available FEM package NASTRAN. For bending vibration, the results are discussed in section 2.1, whereas for inplane vibration they are discussed in section 2.2. For thick plates showing both bending and inplane modes within the first 10 natural frequencies, Carrera's Unified Formulation (CUF) has been used [8–12] for comparison purposes since it provides analytical results in contrast to FE based numerical ones.

The developed theory has been further used to compute the exact natural frequencies and mode shapes of stringer panels (section 3) so as to demonstrate the application of the theory to real structures. The exact results of such structures have never been reported before in the literature. The results from the present theory are also compared with approximate results obtained using NASTRAN. Finally, the efficiency, accuracy and versatility of the DSM when studying the free vibration behaviour of real composite structures are demonstrated.

2. VALIDATION OF RESULTS FOR SIMPLE COMPOSITE PLATES

2.1. Free vibration in bending

The out of plane (or bending) free vibration analysis of a composite square plate is first carried out to validate the theory. The relative material prop-

erties, plate dimensions, and laminate lay-up are as follows: $E_1/E_2 = 40$, $h/a = 0.1$, $a = b = 1m$, $G_{12} = G_{13} = 0.6E_2$, $G_{23} = 0.5E_2$, $\nu_{12} = 0.25, k = 5/6$, lay-up = $[0/90/0]$.

The first 6 natural frequencies of the plate are shown in Table 1 for different boundary conditions (S simply supported, C clamped, F free). The dimensionless natural frequency parameter ($\omega^* = \omega\, a^2/h\sqrt{\rho/E_2}$) together with the corresponding semi-wavelength numbers (m and n) are given and the results are compared with those available in the literature [21, 22] for validation purposes. Approximate results obtained using CQUAD4 NASTRAN elements are also shown. The comparative exact results from the literature [21, 22] are based on the so-called classical method (CM) which uses a Navier's or Levi's type solution and imposes zero or non-zero boundary conditions for displacements and/or forces. This approach can only be used to solve simple plates and cannot be easily extended to structures with complex geometry unlike the DSM. In Table 1, it can be seen that there is total agreement between the solution obtained using DySAP and the exact results reported in the literature [21, 22] in which only the first three natural frequencies are quoted. It can also be observed in Table 1 that NASTRAN consistently produces conservative estimate of the natural frequencies with errors ranging from -0.3 to -6.2% on the first 6 natural frequencies. Understandably, the error would increase for higher natural frequencies. This can be attributed to the fact that the FEM gives an approximate solution for the total elastic energy and since a higher energy is associated with higher modes, a greater error is expected. In Figure 1 some representative modes obtained by using DySAP are compared with those obtained from the FEM analysis. It can

5

be seen that there is excellent agreement between the FE results and the DySAP ones. It should be noted that DySAP results are mesh independent and the mesh used in Figure 1 is merely a plotting grid for convenience.

Further validation cases can be found in Table 2 where a simply supported

Table 1: First 6 dimensionless bending frequencies $\omega^* = \omega\, a^2/h\sqrt{\rho/E_2}$ for a square composite plate with different boundary conditions. Exact results from [21, 22]. FEM results by NASTRAN (mesh 50×50 CQUAD4 elements). DySAP results are mesh independent. Some of the frequencies have been either not shown (n/s) or missed (m) in the published literature.

	SSSS				SSSC			
	Exact [21]	DySAP		FEM	Exact [21]	DySAP		FEM
Mode	ω^*	m n	ω^*	ω^* (error %)	ω^*	m n	ω^*	ω^* (error %)
1	14.766	1 1	14.766	14.716 (-0.3)	17.175	1 1	17.175	17.059 (-0.7)
2	22.158	2 1	22.158	21.718 (-2.0)	23.677	2 1	23.676	23.241 (-1.8)
3	36.900	3 1	36.900	34.945 (-5.3)	37.720	3 1	37.720	35.814 (-5.1)
4	n/s	1 2	37.380	37.072 (-0.8)	n/s	1 2	38.326	37.976 (-0.9)
5	n/s	2 2	41.158	40.728 (-1.0)	n/s	2 2	41.942	41.495 (-1.1)
6	n/s	3 2	50.896	49.268 (-3.2)	n/s	3 2	51.461	49.853 (-3.1)
	SCSC				SFSF			
	Exact [21]	DySAP		FEM	Exact [22]	DySAP		FEM
Mode	ω^*	m n	ω^*	ω^* (error %)	ω^*	m n	ω^*	ω^* (error %)
1	19.669	1 1	19.669	19.490 (-0.9)	4.343	1 1	4.343	4.302 (-0.9)
2	25.349	2 1	25.349	24.915 (-1.7)	missed	1 2	6.262	6.201 (-1.0)
3	38.650	3 1	38.650	36.795 (-4.8)	16.212	2 1	16.212	15.675 (-3.3)
4	n/s	1 2	39.082	38.700 (-1.0)	missed	2 2	18.175	17.619 (-3.1)
5	n/s	2 2	42.585	42.125 (-1.1)	missed	1 3	30.340	30.307 (-0.1)
6	n/s	3 2	51.938	50.347 (-3.1)	33.186	3 1	33.186	31.121 (-6.2)
	SSSF				SFSC			
	Exact [22]	DySAP		FEM	Exact [22]	DySAP		FEM
Mode	ω^*	m n	ω^*	ω^* (error %)	ω^*	m n	ω^*	ω^* (error %)
1	4.914	1 1	4.914	4.869 (-0.9)	7.331	1 1	7.331	7.296 (-0.5)
2	16.742	2 1	16.742	16.200 (-3.2)	17.558	2 1	17.557	17.045 (-2.9)
3	missed	1 2	21.670	21.627 (-0.2)	missed	1 2	23.172	23.066 (-0.5)
4	missed	2 2	27.881	27.499 (-1.4)	missed	2 2	28.961	28.566 (-1.4)
5	33.644	3 1	33.644	31.579 (-6.1)	34.019	3 1	34.019	31.981 (-6.0)
6	n/s	3 2	41.057	39.220 (-4.5)	n/s	3 2	41.721	39.918 (-4.3)

square plate is used as an example. The material properties and dimensions of the plate are: $G_{12} = G_{13} = 0.6E_2$, $G_{23} = 0.5E_2$, $\nu_{12} = 0.25$,$k = 5/6$, lay-up $= [0/90/90/0]$, $h/a = 0.2$, $a = b = 1m$. Separate analyses have been carried out for different Young's modulus ratios E_1/E_2 and the exact results
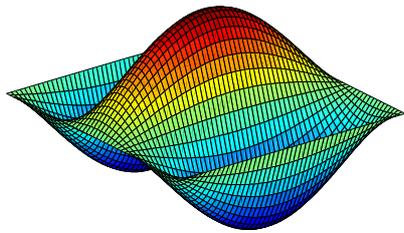
(a) DySAP SSSS mode 3
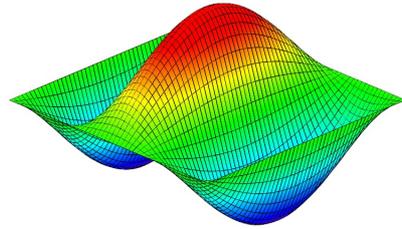
(b) FEM SSSS mode 3
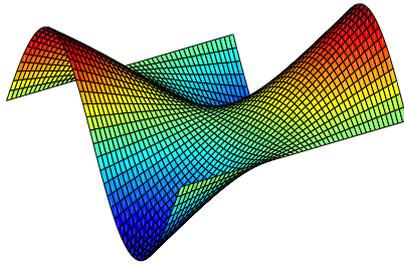
(c) DySAP SFSF mode 4
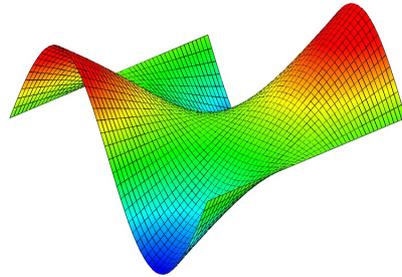
(d) FEM SFSF mode 4
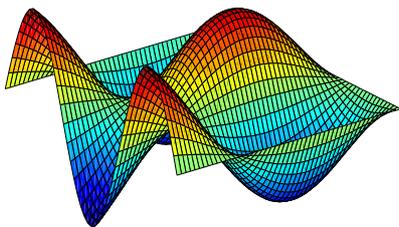
(e) DySAP SFSC mode 6
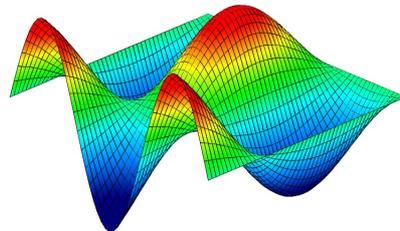
(f) FEM SFSC mode 6

Figure 1: Comparison of some representative mode shapes obtained by DySAP or FEM (NASTRAN) for different boundary conditions.

obtained by DySAP are compared with those reported in [23] using the CM. The FE analysis results computed by NASTRAN are also shown in Table 2. The results obtained by DySAP are in total agreement with those given in [23] whilst the error in the FEM gets progressively higher for increasing Young's modulus ratios.

Next analysis was carried on the same plate with a Young's modulus ratios

Table 2: First dimensionless bending frequencies $\omega^* = \omega\, a^2/h\sqrt{\rho/E_2}$ for a simply supported square composite plate with different Young's modulus ratios. Exact results from [23]. FEM results by NASTRAN (mesh 50×50 CQUAD4 elements). DySAP results are mesh independent.

E_1/E_2	Exact CPT	Exact FSDT	DySAP	FEM (error %)
			ω^*	
10	10.65	8.2982	8.2981	8.350 (0.6)
20	13.948	9.5671	9.5671	9.526 (-0.4)
30	16.605	10.326	10.326	10.196 (-1.3)
40	18.891	10.854	10.854	10.641 (-2.0)

of $E_1/E_2 = 40$ and with different thickness ratios h/a. The results are shown in Table 3. A very small discrepancy can be seen between DySAP results and the exact results reported in [21, 24]. This discrepancy is most likely to be due to a lower number of significant figures used for rounding the results in [21, 24]. This rounding off error assumption seems justified because the results for $h/a = 0.2$ have also been reported in an independent investigation [23] and shown in Table 2. It can be seen that for $E_1/E_2 = 40$, the exact value for the first non-dimensional natural frequency is 10.854 according to Ref. [23] instead of 10.820 of Ref. [21, 24]. Also for this case, it can be seen from Table 3 results that the FEM gives higher errors for higher thickness ratios.

By observing Tables 1, 2, 3, it can be seen that the FEM results are con-

Table 3: First dimensionless bending frequencies $\omega^* = \omega\, a^2/h\sqrt{\rho/E_2}$ for a simply supported square composite plate for different thickness ratios. Exact results from [21, 24]. FEM results by NASTRAN (mesh 50×50 CQUAD4 elements). DySAP results are mesh independent.

h/a	Exact CPT	Exact FSDT	DySAP	FEM (error %)
		ω^*		
0.5	15.830	5.492	5.500	5.134 (-6.7)
0.25	17.907	9.369	9.395	9.117 (-3.0)
0.2	18.215	10.820	10.854	10.641 (-2.0)
0.1	18.652	15.083	15.143	15.086 (-0.4)
0.05	18.767	17.583	17.660	17.647 (-0.1)
0.04	18.780	17.991	18.071	18.061 (-0.1)

sistently lower than the exact ones obtained by DySAP. The latter has been validated against exact results from the literature (obtained using the CM). The anomaly can be explained by the fact that CQUAD4 finite elements in NASTRAN use reduced integration to compute the stiffness matrix of the element in order to avoid the shear locking problem which generally affects thin plates. Reduced integration is used to solve this problem by reducing the precision of the integration on the surface of the element which lead to a lower element stiffness. The user has no control over the type of integration used in CQUAD4 elements and this particular feature is not mentioned in NASTRAN user's guide. Nevertheless, the reduced integration is the most likely cause for FEM giving a lower frequency, i.e. a lower stiffness. Clearly, the FEM should overestimate the stiffness, and if the element is subjected to shear locking, the plate will be much stiffer than what it actually is. This reduced stiffness is what really caused a lower frequency when compared with the exact one. This assertion is further strengthened by observing the fact that the error is much higher for thicker plates (Table 3). Thick plates are not generally subjected to shear locking problems so the reduced integration

9

merely leads to a less accurate stiffness matrix and thus to higher errors.

It should be noted that the shear locking is basically a numerical problem which affects thin FE plates. DySAP and the DSM are strictly speaking not numerical methods since the equations of motions are solved in strong/closed form and thus the results are not affected by shear locking.

2.2. In-plane free vibration

Apparently not much attention has been paid to in-plane or membrane mode vibration of plates in the literature as opposed to bending vibration. Although inplane free vibration for isotropic plates has been studied in some isolated papers [2,5,6], no analytical exact results for composite plates can be found in the literature. In this section the first five in-plane natural frequencies of a square plate are given in Tables 4, 5 and 6 for several combination of boundary conditions. The material properties and dimensions of the plate are: $E_1/E_2 = 40$, $h/a = 0.1$, $a = b = 1m$, $G_{12} = G_{13} = 0.6E_2$, $G_{23} = 0.5E_2$, $\nu_{12} = 0.25$, $k = 5/6$, lay-up = [0/90/0]. It should be noted that with regard to in-plane boundary condition, a distinction between two simply supported (S) cases should be made, namely S1 and S2. The difference between these boundary conditions has been explained in [20] and can be summarised as: S1 (for $y = 0$ and $y = L \Rightarrow u = 0$ and $v \neq 0$; for $x = 0$ and $x = b \Rightarrow v = 0$ and $u \neq 0$) and S2 (for $y = 0$ and $y = L \Rightarrow v = 0$ and $u \neq 0$; for $x = 0$ and $x = b \Rightarrow u = 0$ and $v \neq 0$).

In Table 4 the results are reported for a plate where at least two opposite sites are S1. It can be seen that the first five natural frequencies are dominated by modes with $m = 0$ which cannot be detected by the theory given in the existing DSM literature [6]. It should also be noted that the FE re-

sults obtained by using membrane elements in NASTRAN are surprisingly accurate with an error of less than 0.3%.

Next, in Table 5 the results are reported for a plate where at least two opposite sides S2. With this boundary conditions, the modes corresponding to $m = 0$ are relatively fewer within the first five natural frequencies. Also in this case, NASTRAN results are indeed very accurate.

In Table 6 the results for the remaining combination of boundary conditions are shown. The first five natural frequencies are dominated by $m = 0$ modes. The FEM results are again very accurate.

For illustrative purposes, some representative modes computed by DySAP are compared with those obtained from FEM analysis for different boundary conditions. These are shown Figure 2. It can be seen that the modes are generally in good agreement.

Table 4: First five in-plane natural frequencies $\omega^* = \omega\, a^2/h\sqrt{\rho/E_2}$ for a square composite plate with at least two opposite sides S1-S1. FEM with NASTRAN (mesh 50×50 CQUAD4 elements). DySAP results are mesh independent.

| | S1S1S1S1 | | | | S1S1S1C | | | | S1CS1C | | | |
| | DySAP | | | FEM | DySAP | | | FEM | DySAP | | | FEM |
Mode	m	n	ω^*	ω^* (error %)	m	n	ω^*	ω^* (error %)	m	n	ω^*	ω^* (error %)
1	1	1	24.3	24.3 (0.0)	0	1	24.3	24.3 (0.0)	0	1	24.3	24.3 (0.0)
2	0	1	24.3	24.3 (0.0)	0	2	48.7	48.6 (-0.1)	0	2	48.7	48.6 (-0.1)
3	2	1	48.7	48.6 (-0.1)	0	3	73.0	72.9 (-0.1)	0	3	73.0	72.9 (-0.1)
4	0	2	48.7	48.6 (-0.1)	1	1	85.1	85.1 (0.0)	0	4	97.3	97.1 (-0.3)
5	3	1	73.0	72.9 (-0.1)	2	1	95.0	94.9 (-0.1)	1	1	120.1	120.0 (0.0)
	S1FS1F				S1FS1S1				S1FS1C			
	DySAP			FEM	DySAP			FEM	DySAP			FEM
Mode	m	n	ω^*	ω^* (error %)	m	n	ω^*	ω^* (error %)	m	n	ω^*	ω^* (error %)
1	1	1	22.6	22.6 (0.0)	0	1	12.2	12.2 (0.0)	0	1	12.2	12.2 (0.0)
2	0	1	24.3	24.3 (0.0)	1	1	23.5	23.5 (0.0)	0	2	36.5	36.5 (0.0)
3	2	1	47.0	47.0 (0.0)	0	2	36.5	36.5 (0.0)	0	3	60.8	60.8 (-0.1)
4	0	2	48.7	48.6 (-0.1)	2	1	47.8	47.8 (0.0)	1	1	84.5	84.5 (0.0)
5	3	1	71.3	71.3 (-0.1)	0	3	60.8	60.8 (-0.1)	0	4	85.2	85.0 (-0.2)

Table 5: First five in-plane natural frequencies $\omega^* = \omega\, a^2/h\sqrt{\rho/E_2}$ for a square composite plate with at least two opposite sides S2-S2. FEM with NASTRAN (mesh 50×50 CQUAD4 elements). DySAP results are mesh independent.

		S2S2S2S2				S2S2S2C				S2CS2C			
	DySAP			FEM	DySAP			FEM	DySAP			FEM		
Mode	m	n	ω^*	ω^* (error %)	m	n	ω^*	ω^* (error %)	m	n	ω^*	ω^* (error %)
1	1	1	117.6	117.6 (0.0)	1	1	118.2	118.2 (0.0)	1	1	120.1	120.0 (0.0)
2	1	2	119.9	119.8 (0.0)	1	2	123.0	122.9 (-0.1)	1	2	127.1	126.9 (-0.1)
3	1	3	127.2	127.0 (-0.1)	1	3	132.3	132.0 (-0.2)	1	3	138.4	138.0 (-0.3)
4	1	4	138.3	138.0 (-0.3)	1	4	145.1	144.6 (-0.4)	1	4	152.5	151.9 (-0.4)
5	1	5	152.6	151.9 (-0.4)	1	5	160.6	159.7 (-0.5)	0	1	163.4	163.3 (0.0)
		S2FS2F				S2FS2S2				S2FS2C			
	DySAP			FEM	DySAP			FEM	DySAP			FEM		
Mode	m	n	ω^*	ω^* (error %)	m	n	ω^*	ω^* (error %)	m	n	ω^*	ω^* (error %)
1	1	1	22.6	22.6 (0.0)	0	1	81.7	81.7 (0.0)	0	1	81.7	81.7 (0.0)
2	2	1	47.0	47.0 (0.0)	1	1	84.5	84.4 (0.0)	1	1	84.5	84.5 (0.0)
3	3	1	71.3	71.3 (-0.1)	2	1	94.1	94.0 (-0.1)	2	1	94.1	94.0 (-0.1)
4	4	1	95.7	95.5 (-0.2)	3	1	108.4	108.1 (-0.2)	3	1	1108.4	108.1 (-0.2)
5	1	2	117.6	117.6 (0.0)	1	2	117.6	117.6 (0.0)	1	2	1118.3	118.2 (0.0)

Table 6: First five in-plane natural frequencies $\omega^* = \omega\, a^2/h\sqrt{\rho/E_2}$ for a square composite plate with S1-S2-S1-S2. FEM with NASTRAN (mesh 50×50 CQUAD4 elements). DySAP results are mesh independent.

		S1S2S1S2		
	DySAP			FEM
Mode	m	n	ω^*	ω^* (error %)
1	0	2	24.3	24.3 (0.0)
2	0	3	48.7	48.6 (-0.1)
3	0	4	73.0	72.9 (-0.1)
4	0	5	97.3	97.1 (-0.3)
5	1	1	117.6	119.8 (1.9)

(a)   DySAP S1S1S1S1 mode 3

(b)   FEM S1S1S1S1 mode 3

(c)   DySAP S1FS1C mode 1

(d) FEM S1FS1C mode 1

(e)   DySAP S2S2S2S2 mode 2

(f)   FEM S2S2S2S2 mode 2

(g) DySAP S2FS2F mode 2

(h) FEM S2FS2F mode 2
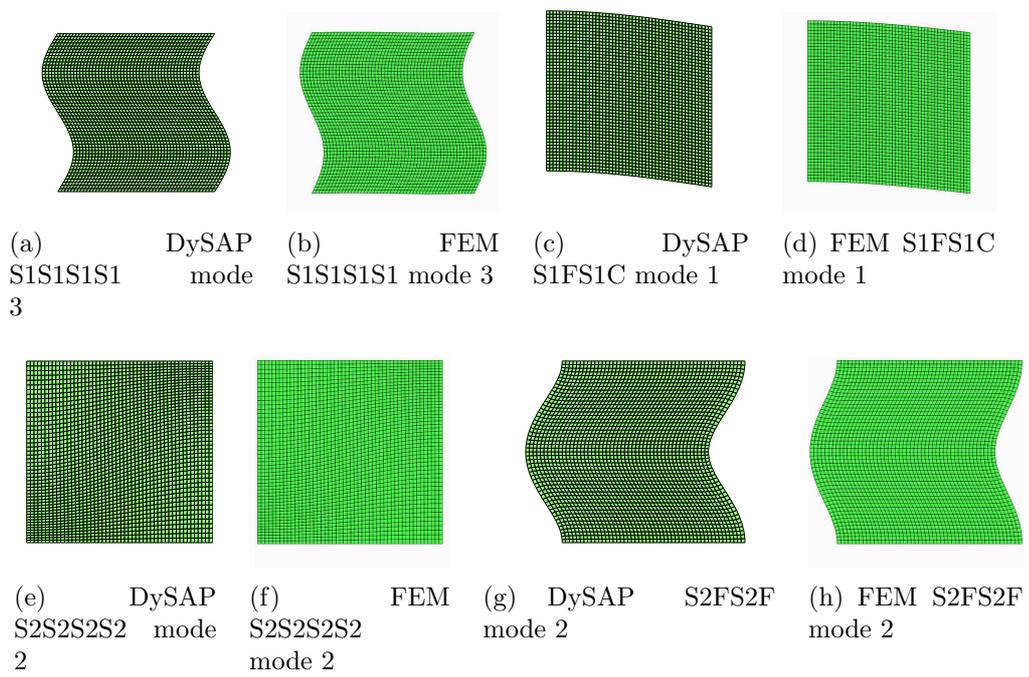
Figure 2: Mode comparison between DySAP and FEM (NASTRAN)

2.3. Vibrations of think plates

A relatively thick square composite plate, simply supported on its four sides (S2-S2-S2-S2), is the final validation example presented for simple plates. The plate material properties and geometry are: $E_1/E_2 = 10$, $E_1 = 110$ GPa, $G_{12} = G_{13} = 0.6E_2$, $G_{23} = 0.5E_2$, $\nu_{12} = 0.25$, $k = 5/6$, lay-up = $[0/90/90/0]$, $h/a = 0.2$, $a = b = 1m$. The results from the DySAP analysis are reported in Table 7. Only the first natural frequency could be found in the literature [21, 22] that was obtained by using Navier type exact approach. DySAP results are also compared with those obtained by using Carrera's Unified Formulation (CUF) [8–12, 16, 17] as well as by using a finite element model consisting of 100×100 plate elements solved by NASTRAN. The number of semi-wavelengths of the modes is also reported (m and n) in the table along with an indication of whether the mode is a bending (b) or in-plane (p) or an in-plane with $m = 0$ (m) mode. Two different analyses have been carried out by using the CUF. In CUF (a) an equivalent single layer elements of the first order (referred to as ED1 [8–12, 16, 17]) with corrections needed for an FSDT formulation has been used. In CUF (b) the same element has been used but a further correction on the constitutive model (C_{13}, C_{23}, $C_{33} = 0$ [16, 17]) has been added to remove all of the out of plane effects to make the ED1 model to resemble as close as reasonably possible to the FSDT so that a direct comparison can be made. By comparing DySAP and CUF (b) results, it can be observed that there is complete agreement between the two sets of results with the only exception that the Navier's solution for $m = 0$ is missed by CUF solution. If CUF (a) results are used instead for comparison, it can be seen that there

14

is minor disagreements between the frequencies for in-plane modes 16, 18, 19. This is due to the fact that CUF (a) (which uses ED1 elements) takes the deformability through the thickness into account which makes the plate slightly less stiff than the FSDT formulation, thus giving rise to lower natural frequencies.

From the comparison made between DySAP, CUF and the CM results, it can be generally concluded that DySAP results are correct and thus they can be used as a benchmark to validate approximate solutions.

The last columns of Table 7 show the results computed using NASTRAN along side the DySAP results. There is good agreement in general between the approximate FEM results and the exact DySAP results with a maximum error of about 6%, occurring for the 20th natural frequency. Comparing DySAP and FEM results, the following further comments on the FEM results can be made. (i) In plane natural frequencies show a relatively lower error than the bending natural frequencies, (ii) The error generally increases for higher natural frequencies, (iii) The error increases more rapidly with the m values of the semi-wavelength rather than the n, which could be due to the particular lay-up chosen for the laminate, (iv) The order of the modes given by the FEM may be erroneous on occasions due to errors which are different from mode to mode and have no direct bearing on the mode number. For instance, the 6th FE mode is not really the 6th as DySAP results show, but it is actually the 7th and the 7th FEM mode is actually the 6th. The same situation is apparent for modes 9 and 10 and also for 20 and 21.

Next, a comparison between some computed DySAP and NASTRAN modes is shown in Figure 3 for bending free vibration and in Figure 4 for inplane

free vibration. From these figures it can be observed that the mode shapes are generally in good agreement. The modal interchange observed previously as explained in (iv) above can also be observed in Figures 3(e)-3(f), 3(g)-3(h) and 4(a)-4(b).

Table 7: First 21 dimensionless natural frequencies $\omega^* = \omega\, a^2/h\sqrt{\rho/E_2}$ for a simply supported (S2-S2-S2-S2) square plate. CS (classical solution) [21, 22], CUF (Carrera's Unified Formulation). The mode shapes are distinguished by in-plane (p), bending (b) and the in-plane special case m=0 (m).

	CS	CUF (a)	CUF (b)	DySAP				FEM, NASTRAN			
Mode	ω^*	ω^*	ω^*	type	m	n	ω^*	type	m	n	ω^* (error %)
1	8.30	8.30	8.30	b	1	1	8.30	b	1	1	8.35 (0.7)
2	/	15.30	15.30	b	2	1	15.30	b	2	1	15.09 (-1.4)
3	/	18.87	18.87	b	1	2	18.87	b	1	2	18.99 (0.6)
4	/	23.13	23.13	b	2	2	23.13	b	2	2	23.09 (-0.2)
5	/	25.32	25.32	b	3	1	25.32	b	3	1	24.34 (-3.8)
6	/	30.02	30.02	b	1	3	30.02	b	3	2	30.06 (0.1)
7	/	30.84	30.84	b	3	2	30.84	b	1	3	30.10 (-2.4)
8	/	32.99	32.99	b	2	3	32.99	b	2	3	33.01 (0.1)
9	/	36.10	36.10	p	1	1	36.10	b	4	1	34.17 (-5.4)
10	/	36.25	36.25	b	4	1	36.25	p	/	/	36.10 (-0.4)
11	/	/	/	p	1	2	36.95	p	/	/	36.95 (0.0)
12	/	/	/	m	0	1	36.95	m	/	/	36.95 (0.0)
13	/	38.84	38.84	b	3	3	38.84	b	3	3	38.24 (-1.6)
14	/	40.37	40.37	b	4	2	40.37	b	4	2	38.46 (-4.7)
15	/	41.06	41.06	b	1	6	41.06	b	1	6	41.06 (0.0)
16	/	40.71	41.52	p	1	3	41.52	p	/	/	41.51 (0.0)
17	/	43.35	43.35	b	2	4	43.35	b	2	4	43.36 (0.0)
18	/	43.47	43.70	p	1	4	43.70	p	/	/	43.69 (0.0)
19	/	43.48	43.70	p	2	1	43.70	p	/	/	43.69 (0.0)
20	/	46.79	46.79	b	4	3	46.79	b	5	1	44.03 (-5.9)
21	/	47.42	47.42	b	5	1	47.42	b	4	3	45.10 (-4.9)

(a) DySAP mode 1

(b) FEM mode 1

(c) DySAP mode 2

(d) FEM mode 2

(e) DySAP mode 6

(f) FEM mode 7

(g) DySAP mode 21

(h) FEM mode 20
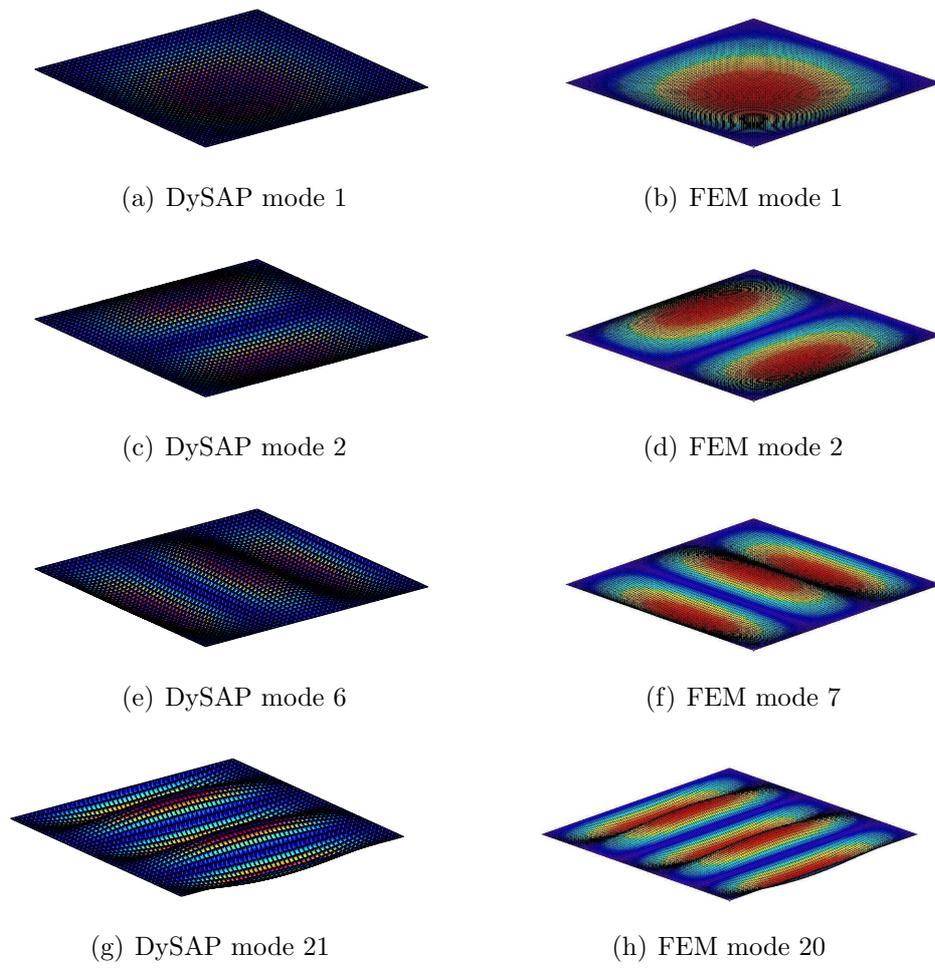
Figure 3: Comparison of some bending modes between DySAP and FEM (NASTRAN) for a simply supported (S2-S2-S2-S2) square composite plate.

17
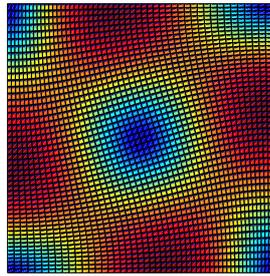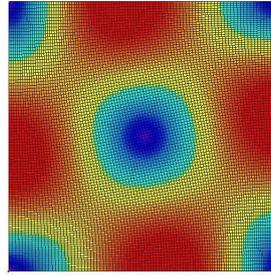
(a) DySAP mode 9   (b) FEM mode 10
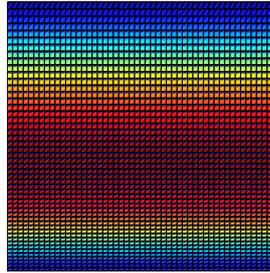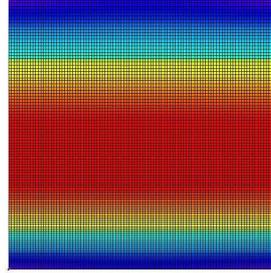
(c) DySAP mode 11   (d) FEM mode 11

Figure 4: Comparison of some in-plane modes between DySAP and FEM (NASTRAN) for a simply supported (S2-S2-S2-S2) square composite plate.

3. PRACTICAL STRUCTURES

The dynamic stiffness formulation for composite plate elements based on the first order shear deformation theory developed in Part I of this paper and implemented in the computer program DySAP has so far been extensively validated for simple plates. The advantages of the method when compared to the classical Navier's solution have not yet been highlighted. Navier's solution is applicable only to simple individual plates while the dynamic stiffness method (DSM) being more versatile can obtain the exact solution of any structure that can be modelled as an assembly of plates. An interesting feature of the DSM is that the results are independent of the number of element used in the analysis. A single element can be used to model any part of the structure which can be idealised as a uniform single plate[1]. In this case, with a limited number of elements, any number of natural frequencies can be computed for a complex structure by assembling the individual structures in an exact sense to achieve a desired accuracy. The solution from the DSM can be used as benchmark to validate approximate numerical methods, but importantly can be exploited for several applications in design. In fact, the most commonly used method to solve free vibration problems is acknowledge to be the finite element method (FEM) since it can handle complex geometries. The FEM, versatile though it is, is generally inaccurate at high frequencies and is numerically as well as computationally inefficient when compared with the DSM. In the following sections some representative real structures are

---

[1]The use of a single element will likely trigger j_0 in the Wittrik and Williams' algorithm which could cause additional complications (see [20]). Moreover, if the element is geometrically big, some components of the stiffness matrix could cause numerical problems. Thus, sometimes more than 1 element might be needed.

analysed to illustrate the potential of the DSM in terms of both accuracy and computational time.

Two plates reinforced by stiffeners are taken as examples. The first one has an L stringer and the second one has an omega stringer . It should be noted that no exact solution for such complex composite structures has ever been reported in the literature to the best of the authors' knowledge.

3.1. L stringer panel

The geometry of the plate with an L stringer is shown in Figure 5. The skin is a square plate 1 m × 1 m and the stringer is placed in the middle of the plate. The web of the stringer is 0.2 m high and its flange is 0.1 m wide. The thickness of each plate is kept constant for the whole structure and two different thickness ratios have been used, namely $h/a = 0.001$ and $h/a = 0.005$ when obtaining the results. The material properties used are: $E_1/E_2 = 40$, $G_{12} = G_{13} = 0.6E_2$, $G_{23} = 0.5E_2$, $\nu_{12} = 0.25, k = 5/6$. The laminate lay-up is [0/90/90/0]. The overall structure is simply supported on all its sides (S1-S1-S1-S1). The first 20 dimensionless natural frequencies computed using DySAP are shown in Table 8. The exact results obtained by DySAP are compared with those obtained by the FEM. An FE model with 3250 square plate elements (CQUAD4) was built and the first 20 natural frequencies were computed using NASTRAN. By contrast DySAP results are mesh independent and the number of elements used in the analysis is not important when computing the natural frequencies. These are also shown in Table 8. As can be seen, the NASTRAN results are consistently accurate with a maximum error of just 1%. Some representative modes obtained by DySAP and NASTRAN are compared in Figure 6. It can be seen that

20

there is excellent agreement between the two sets of mode shapes (Figures 6(a)-6(b) for global modes) and (Figures 6(c), 6(d), 6(e) and 6(f) for local modes).

Although it might appear that there is no clear advantage of using DySAP instead of using a commercial FE solver such as NASTRAN in terms of accuracy of results in this case, a different picture emerges when viewed in terms of analysis time. Referring to Table 9, it can be seen that the dynamic stiffness method implemented in DySAP is much more computationally efficient. Although DySAP has not been optimised neither in terms of memory storage nor in terms of solution technique, it is still 15 times faster than NASTRAN when computing just one natural frequency. This is significant, particulary when carrying out optimisation studies where repetitive sensitivity calculations contribute quite heavily to the overall simulation time. This difference in computational time is mainly due to the large number of finite elements necessary to obtain an accurate solution using NASTRAN. When a larger number of frequencies is needed, due to the very nature of the Wittrick and Williams algorithm, the computational time will increase. DySAP is still seen to be 8 times faster than NASTRAN when computing the first 25 natural frequencies. An advantage of the Wittrick and Williams algorithm is that it is easy to compute only the required natural frequency or natural frequencies in any arbitrary order. This means that if only the 87th frequency of the structure is required, the time needed will be more or less the same as computing only the first natural frequency and the accuracy of the solution will not be affected anyway.
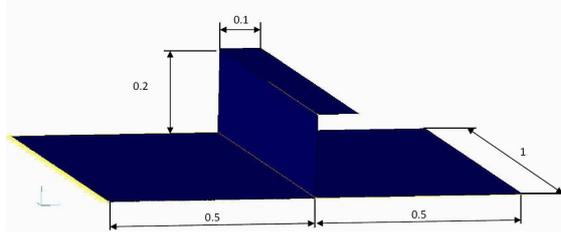
Figure 5: Geometry of the L stringer composite panel. (Dimensions in metre)

Table 8: First 20 dimensionless natural frequencies $\omega^* = \omega\, a^2/h\sqrt{\rho/E_2}$ for a simply supported (S1-S1-S1-S1) composite plate reinforced by an L-shaped stringer. The results have been obtained by DySAP and NASTRAN for two different thickness ratios.

| | $h/a = 0.001$ | | $h/a = 0.005$ | |
| | DySAP | FEM | DySAP | FEM |
Mode	ω^*	ω^* (error %)	ω^*	ω^* (error %)
1	83.3	83.3 (0.0)	81.5	81.5 (0.0)
2	89.3	89.1 (-0.1)	88.6	88.5 (-0.1)
3	106.1	106.1 (0.0)	100.5	100.4 (0.0)
4	107.6	107.3 (-0.3)	107.1	106.8 (-0.3)
5	111.1	110.9 (-0.1)	109.3	109.1 (-0.1)
6	126.5	126.1 (-0.3)	125.2	124.9 (-0.3)
7	143.6	143.2 (-0.3)	143.1	142.5 (-0.4)
8	158.5	157.9 (-0.4)	157.4	156.8 (-0.4)
9	197.9	197.2 (-0.3)	197.0	196.1 (-0.5)
10	209.1	208.3 (-0.4)	199.1	198.6 (-0.2)
11	268.8	268.0 (-0.3)	207.9	206.8 (-0.5)
12	271.4	270.5 (-0.3)	253.6	252.7 (-0.3)
13	275.4	274.2 (-0.4)	267.4	266.0 (-0.5)
14	277.4	276.4 (-0.4)	270.8	269.5 (-0.5)
15	285.0	283.4 (-0.6)	275.7	274.1 (-0.6)
16	304.6	302.2 (-0.8)	281.3	279.6 (-0.6)
17	329.4	327.1 (-0.7)	290.0	288.9 (-0.4)
18	334.7	331.9 (-0.8)	301.1	298.6 (-0.8)
19	338.2	334.9 (-1.0)	314.4	312.8 (-0.5)
20	340.8	340.2 (-0.2)	327.7	326.4 (-0.4)

Table 9: Comparison of the relative computational times using DySAP (dynamic stiffness method) and NASTRAN (finite element method). The smallest analysis time has been considered as a single unit of time in order to have a comparative analysis.

Method	Number of Elements	Degree of Freedom	Number of modes	Relative real time
DySAP	8	45	1	1.00
DySAP	8	45	25	2.45
FEM	3250	20196	1	15.09
FEM	3250	20196	25	19.69
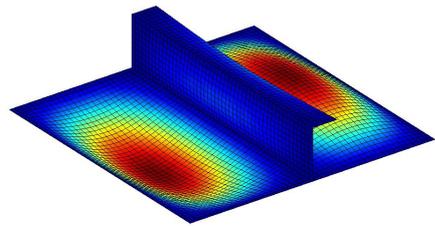
(a) DySAP mode 1
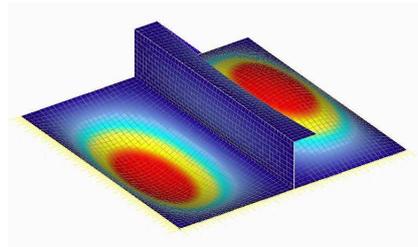
(b) FEM mode 1
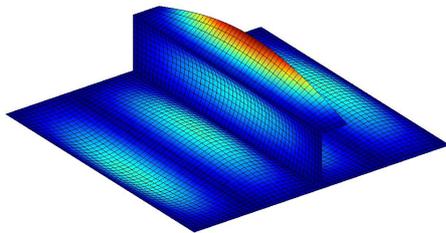
(c) DySAP mode 12
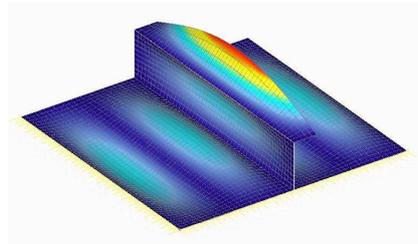
(d) FEM mode 12
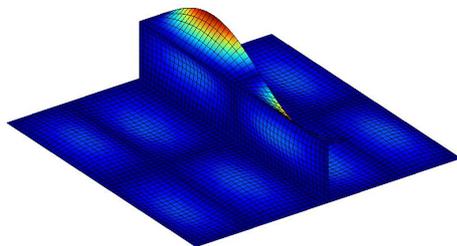
(e) DySAP mode 18
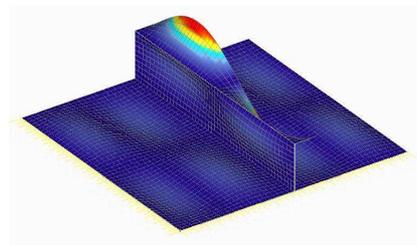
(f) FEM mode 18

Figure 6: Comparison of some modes between DySAP and FEM (NASTRAN) for the composite plate with an L stringer.

3.2. Omega stringer panel

In this section a composite panel with an omega stringer is investigated to show the versatility of the dynamic stiffness method using the program DySAP. The geometry is shown in Figure 7. The outer skin is 1.5 m $\times$ 1.5 m and the omega stringer is centre-adjusted, i.e. it is in the middle, as shown, with the two sides at 45 degrees extending for 0.1 m horizontally and 0.1 m vertically and the central part of the stringer is 0.3 m wide. The material properties are: $E_1/E_2 = 40$, $G_{12} = G_{13} = 0.6E_2$, $G_{23} = 0.5E_2$, $\nu_{12} = 0.25$, $k = 5/6$. The lay-up is $[0/90/90/0]$ and each layer is 0.25 mm thick.

In Table 10 the first 30 dimensionless natural frequencies computed by DySAP and NASTRAN are respectively shown. The finite element model has a fine structured mesh composed of 31200 square elements (CQUAD4). DySAP results are mesh independent and the number of elements used in the analysis is not important when computing the natural frequencies. It can be seen that in the NASTRAN analysis the error increases with increasing natural frequencies. Although the error is very small for the first natural frequency, it reaches 2.1% for higher ones.

In Figure 8 a comparison between some representative modes obtained by DySAP and NASTRAN is shown. The modes computed using DySAP are in good agreement with NASTRAN. In Figures 8(a) and 8(b) the comparison is shown for the first global mode for which the natural frequencies from the two analyses show an appreciable error. In Figures 8(c) and 8(d) the comparison for the first local mode of the stringer is shown. It can be observed that the mode shapes are generally in good agreement.

Table 11 shows comparison of the solution time between DySAP and NAS-TRAN analysis. It can be seen that DySAP is 35 times faster in computing the first natural frequency when compared to NASTRAN. This superiority in terms of computational time and accuracy of results will increase with the complexity of the structure.
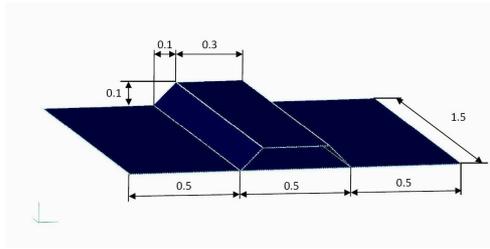
Figure 7: Geometry of the Omega stringer composite panel. (Dimensions in metre)

Table 10: First 30 dimensionless natural frequencies $\omega^* = \omega\, a^2/h\sqrt{\rho/E_2}$ for a simply supported (S1-S1-S1-S1) composite plate reinforced by an omega-shaped stringer.

Mode	DySAP			FEM	Mode	DySAP			FEM
	m	n	ω^*	ω^* (error %)		m	n	ω^*	ω^* (error %)
1	1	1	204.4	204.6 (0.1)	16	6	2	342.5	347.5 (1.5)
2	2	1	208.0	208.3 (0.2)	17	5	3	355.6	358.1 (0.7)
3	1	2	215.9	216.2 (0.1)	18	6	3	401.6	405.9 (1.1)
4	3	1	217.9	218.7 (0.4)	19	7	1	409.0	416.5 (1.8)
5	2	2	220.4	220.7 (0.2)	20	7	2	416.0	423.4 (1.8)
6	3	2	230.0	230.8 (0.3)	21	7	3	466.3	472.8 (1.4)
7	4	1	239.7	241.4 (0.7)	22	8	1	501.6	511.7 (2.0)
8	4	2	250.9	252.5 (0.7)	23	8	2	507.5	517.5 (2.0)
9	5	1	277.7	280.8 (1.1)	24	8	3	549.8	558.9 (1.7)
10	5	2	287.5	290.6 (1.1)	25	9	1	610.8	623.9 (2.1)
11	1	3	294.3	294.6 (0.1)	26	9	2	615.7	628.7 (2.1)
12	2	3	302.1	302.5 (0.1)	27	1	4	633.0	633.5 (0.1)
13	3	3	310.0	310.7 (0.2)	28	9	3	651.4	663.6 (1.9)
14	4	3	326.2	327.5 (0.4)	29	2	4	673.7	674.3 (0.1)
15	6	1	334.1	339.2 (1.5)	30	1	5	678.4	679.0 (0.1)

(a) DySAP mode 9

(b) FEM mode 9

(c) DySAP mode 27

(d) FEM mode 27
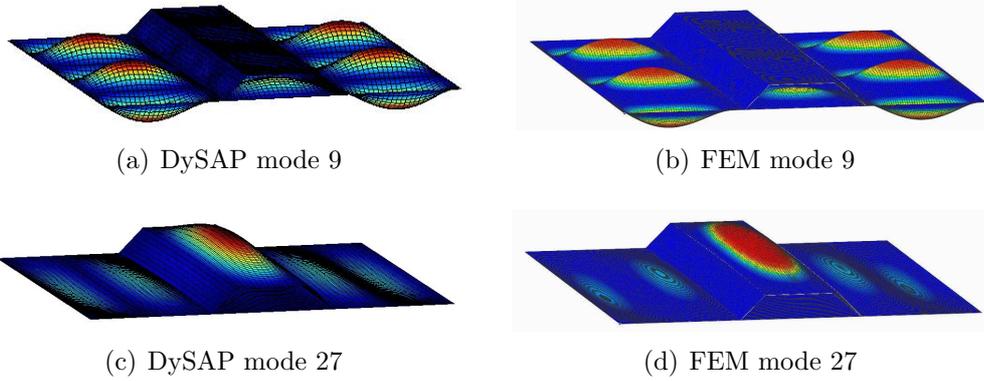
Figure 8: Comparison of some modes between DySAP and FEM (NASTRAN) for the composite plate with an omega stringer.

Table 11: Comparison of the relative computational times using DySAP (dynamic stiffness method) and NASTRAN (finite element method). The smallest analysis time has been considered as a single unit of time in order to have a comparative analysis.

Method	Number of Elements	Degree of Freedom	Number of modes	Relative real time
DySAP	13	65	1	1.00
DySAP	13	65	25	2.72
FEM	31200	188448	1	35.07
FEM	31200	188448	25	49.54

4. CONCLUSIONS

In this second part of the two part paper, the dynamic stiffness formulation for composite plate elements based on the first order shear deformation theory presented in the first part, has been implemented in a computer program called DySAP which has been extensively validated and then used to carry out the free vibration analysis of realistic structures.

Initially only free bending vibration is considered for validation purposes using different boundary conditions and different thickness and Young's modulus ratios. The results are compared with those in the literature and with finite element results obtained by NASTRAN. Subsequently, in-plane free vibration is carried out and the results are compared with finite element results rather than exact results due to their unavailability in the literature for composites. Next, a thicker composite plate which exhibits both in-plane and out of plane vibrational modes between the first twenty is investigated. The results obtained by DySAP have been validated against those in the literature and also against those obtained by using Carrera's Unified Formulation. In all cases, excellent agreement was found. Comparison of DySAP results against NASTRAN shows that if a sufficiently fine mesh in the latter is used, generally the error made by the finite element is small but it increases for higher frequencies, as expected. It has also been noted that FEM may produce results where modes are interchanged.

After extensive validation of the DSM implemented in DySAP with the help of results available in the literature for simple plates, DySAP has then been used to determine for the first time the exact solution for two stringer panels. These results have been compared with finite elements results obtained by

NASTRAN. Judging from the comparison of computational time and bearing in mind that DySAP program has not been optimised for speed, unlike NASTRAN, it can be concluded that the dynamic stiffness method implemented in DySAP is not only more accurate but also much more computationally efficient than the finite element method when carrying out free vibration analysis of plate assemblies. The advantage of computational time gained using DySAP will increase for more complex structures which will require more finite elements for accurate modelling. DySAP analysis will be particulary useful in optimisation studies which are generally computationally intensive.

Although DySAP is much more accurate and computationally efficient, it cannot obviously replace the use of the finite element method because it cannot investigate any geometry with any boundary condition at present. DySAP should be used when at least two sides of the structure are simply supported and importantly, when the structure can be modelled as an assembly of plates. This indicates the need for multi-method software that will use the most accurate and efficient solution procedure for each particular problem without resorting to the finite element method all the time regardless.

Acknowledgements

28

References

[1] J. N. Reddy, Mechanics of laminated composite plates and shells. Theory and analysis, CRC Press, 2004.

[2] Y. F. Xing, B. Liu, Exact solutions for the free in-plane vibrations of rectangular plates, International Journal of Mechanical Sciences 51 (3) (2009) 246–255.

[3] N. S. Bardell, R. S. Langley, J. M. Dunsdon, On the free in-plane vibration of isotropic rectangular plates, Journal of Sound and Vibration 191 (3) (1996) 459–467.

[4] C. I. Park, Frequency equation for the in-plane vibration of a clamped circular plate, Journal of Sound and Vibration 313 (1-2) (2008) 325–333.

[5] D. Gorman, Exact solutions for the free in-plane vibration of rectangular plates with two opposite edges simply supported, Journal of Sound and Vibration 294 (1-2) (2006) 131 – 161.

[6] M. Boscolo, J. R. Banerjee, Dynamic stiffness method for exact inplane free vibration analysis of plates and plate assemblies, Journal of Sound and Vibration 330 (2011) 29282936.

[7] R. L. Woodcock, R. B. Bhat, I. G. Stiharu, Effect of ply orientation on the in-plane vibration of single-layer composite plates, Journal of Sound and Vibration 312 (2008) 94 – 108.

[8] E. Carrera, A study of transverse normal stress effect on vibration of multilayered plates and shells, Journal of Sound and Vibrations 225 (5) (1999) 803–829.

[9] E. Carrera, Layer-wise mixed models for accurate vibration analysis of multilayered plates, Transactions of the ASME 65 (1998) 820–828.

[10] E. Carrera, L. Demasi, M. Manganello, Assessment of plate elements on bending and vibrations of composite structures, Mechanics of Advanced Materials and Structures 9 (2002) 333–357.

[11] E. Carrera, M. Boscolo, Classical and mixed finite elements for static and dynamic analysis of piezoelectric plates, International journal for numerical methods in engineering 70 (2007) 1135–1181.

[12] E. Carrera, M. Boscolo, A. Robaldo, Hierarchic multilayered plate elements for coupled multifield problems of piezoelectric adaptive structures: Formulation and numerical assessment, Archives of computational methods in engineering 14 (2007) 383–430.

[13] J. N. Reddy, Theory and analysis of elastic plates, CRC Press, 2006.

[14] J. N. Reddy, A. Miravete, Practical analysis of composite laminates, CRC Press, 2000.

[15] J. N. Reddy, N. D. Phan, Stability and vibration of isotropic, orthotropic and laminated plates according to a higher-order shear deformation theory, Journal of Sound and Vibrations 98 (2) (1985) 157–170.

[16] F. A. Fazzolari, E. Carrera, Advanced variable kinematics ritz and galerkin formulations for accurate buckling and vibration analysis of anisotropic laminated composite plates, Composite Structures (2011) doi:10.1016/j.compstruct.2011.07.018.

[17] E. Carrera, F. A. Fazzolari, L. Demasi, Vibration analysis of anisotropic simply supported plates by using variable kinematic and rayleigh-ritz method, Journal of Vibration and Acoustics (2011) doi:10.1115/1.4004680.

[18] M. Boscolo, J. R. Banerjee, Dynamic stiffness elements and their applications for plates using first order shear deformation theory, Computers and Structures 89 (2010) 395–410.

[19] O. C. Zienkiewicz, R. L. Taylor, The Finite element method, 5th Edition, Vol. 1: The basis, Butterworth-Heinemann, 2000.

[20] M. Boscolo, R. J. Banerjee, Dynamic stiffness formulation for composite mindlin plates for exact modal analysis of structures. Part I: Theory, Computers and Structures.Under Review.

[21] O. Civalek, Free vibration analysis of symmetrically laminated composite plates with first-order shear deformation theory (FSDT) by discrete singular convolution method, Finite Elements in Analysis and Design 44 (2008) 725–731.

[22] A. A. Khdeir, L. Librescu, Analysis of symmetric cross-ply laminated elastic plates using higher-order theory: Part II - buckling and free vibration, Composite Structures 9 (1988) 259–277.

[23] A. A. Khdeir, Free vibration and buckling of symmetric cross-ply laminated plates by an exact method, Journal of Sound and Vibration 126 (3) (1988) 447–461.

[24] J. N. Reddy, N. D. Phan, Stability and vibration of isotropic, orthotropic and laminated plates according to a higher-order shear deformation theory, Journal of Sound and Vibration 98 (2) (1985) 157–170.